Simulation of induced potentials in bone under ultrasound irradiation

Hidehisa Suzuyama[1‡], Taisei Tsubata[1], Keigo Maehara[1], Atsushi Hosokawa[2], Takao Tsuchiya[1], Ko Chiba[3] and Mami Matsukawa[1] ([1]Doshisha Univ.; [2]NIT, Akashi college; [3]Nagasaki Univ.)

1. Introduction

Low Intensity Pulsed Ultra-Sound (LIPUS) can shorten the healing time of fractures by irradiating ultrasound. However, the initial mechanism of bone fracture healing is still unknown. One possible mechanism is the ultrasonically induced electrical potentials due to the weak piezoelectricity of bone. If electrical potentials are induced, the electrical stimulation may contribute to the fracture healing. There are several studies reporting the acceleration of fracture healing due to electrical stimulation[1, 2, 3].

In this study, a human radius digital model was created for the simulation of ultrasonilcally induced electrical potentials in bone by the PE-FDTD method (eastic FDTD method with piezoelectricity)[4].

2. Model fabrication and FDTD simulation

A 3D digital bone model was created using high-resolution peripheral bone CT (HR - pQCT, Scanco Medical, Xtreme CT II) data of the radius of a 66-year-old woman (**Fig. 1**). The model was heterogeneous. The density of each voxel was in the range of 1700 - 2400 kg/m^3. For comparison, an homogeneious pipe-like bone model with wall thickness of 1.4 mm, length of 74 mm and density of 2000 kg/m^3 was also created. Each model was uniaxially anisotropic along the z axis. Elastic moduli in Eq.1 were calculated from average density 2000 kg/m^3 and wave velocities from references[5, 6, 7]. The piezoelectric constants in Eq. 2 used were from a reference[4].

$$C_{ij} = \begin{pmatrix} 25.3 & 12.5 & 12.8 & 0 & 0 & 0 \\ 12.5 & 25.3 & 12.8 & 0 & 0 & 0 \\ 12.8 & 12.8 & 35.3 & 0 & 0 & 0 \\ 0 & 0 & 0 & 8.8 & 0 & 0 \\ 0 & 0 & 0 & 0 & 8.8 & 0 \\ 0 & 0 & 0 & 0 & 0 & 6.4 \end{pmatrix} \text{[GPa]} \quad (1)$$

$$e_{ij} = \begin{pmatrix} 0 & 0 & 0 & 10 & 2 & 0 \\ 0 & 0 & 0 & 2 & -10 & 0 \\ 0.15 & 0.15 & 0.15 & 0 & 0 & 0 \end{pmatrix} \text{[mC/m}^2\text{]} \quad (2)$$

The spatial and temporal resolutions of the simulations were 61 μm and 8 ns, respectively. Higdon's second-order absorbing boundary condition was used in the simulation. The transmitter (diameter: 10 mm) was set at 90° (normal incidence of sound) or 45° to the bone surface as shown in Fig.1 (b). The x-axis is the radial direction, the y-axis is the tangential direction, and the z-axis is the bone axis. The radiated wave from the transmitter was one cycle of sinusoidal wave at 1 MHz with Hann window.

In the PE-FDTD method, a motion equation and piezoelectric constitutive equations used are as follows:

$$\rho \frac{\partial u_i}{\partial t} = \frac{\partial T_{ii}}{\partial i} + \frac{\partial T_{ij}}{\partial j} + \frac{\partial T_{ik}}{\partial k} \quad (3)$$

$$\frac{\partial T_{ii}}{\partial t} + r_n T_{ii} = C_{ii}\frac{\partial u_i}{\partial i} + C_{ij}\frac{\partial u_j}{\partial j} + C_{ik}\frac{\partial u_k}{\partial k} - e_{ii}\frac{\partial E_i}{\partial t} - e_{ji}\frac{\partial E_j}{\partial t} - e_{ki}\frac{\partial E_k}{\partial t} \quad (4)$$

$$\frac{\partial T_{jk}}{\partial t} + r_s T_{ii} = C_{li}\frac{\partial u_i}{\partial i} + C_{lj}\frac{\partial u_j}{\partial j} + C_{lk}\frac{\partial u_k}{\partial k} - e_{il}\frac{\partial E_i}{\partial t} - e_{jl}\frac{\partial E_j}{\partial t} - e_{kl}\frac{\partial E_k}{\partial t} \quad (5)$$

$$\epsilon_{ii}\frac{\partial E_i}{\partial t} = -e_{ii}\frac{\partial u_i}{\partial i} - e_{ij}\frac{\partial u_j}{\partial j} - e_{ik}\frac{\partial u_k}{\partial k} - \frac{e_{il}}{2}\left(\frac{\partial u_j}{\partial k} + \frac{\partial u_k}{\partial j}\right) - \frac{e_{im}}{2}\left(\frac{\partial u_k}{\partial i} + \frac{\partial u_i}{\partial k}\right) - \frac{e_{in}}{2}\left(\frac{\partial u_i}{\partial j} + \frac{\partial u_j}{\partial i}\right) - \sigma_i E_i \quad (6)$$

Here, i,j,k = 1,2,3, (x,y,z), and l,m,n = 4,5,6, (yz, zx, xy), respectively. u is the particle velocity, Tii is the normal stress, Tjk ($j \neq k$) is the shear stress, Ei is the electric field. Moreover, ρ is the density, ϵii is the dielectric constant and σi is the conductivity. We referred the attenuation from bovine bone data. The attenuation of longitudinal (r_n) waves was 2.1 dB/cm/MHz in the axial (load) direction and 3.1 dB/cm/MHz in the off-axis directions[8]. The shear wave attenuation (r_s) was assumed to be 5.2 dB/cm/MHz[9].

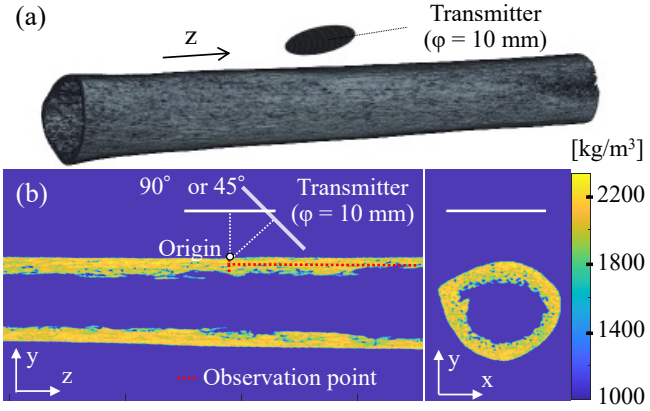

Fig. 1 A human radius bone model.

3. Results and Discussion

In the case of normal incidence (90°) to the pipe model (Fig. 2), the radiated ultrasound from the edge of the transmitter entered the bone obliquely, which

generated weak shear waves. This shear wave reached just below the sensor, generating weak ***Ex***. In the case of normal incidence (90°) to the bone model, shear waves were generated at the surface due to the surface irregularity and slightly deflection shape. In the case of 45° incidence, which was higher than the critical angle of the longitudinal wave, shear waves mainly propagated, and strong ***Ex*** was generated.

The electric field in the bone was highly dependent on the shear stress, as shown in Eq. 2. **Figure 2** also shows the waveforms of the measurement points along the y axis direction inside the bone model.

Figures 3 and 4 show the maximum field strength $\boldsymbol{E}$ (= ($\boldsymbol{Ex}^2 + \boldsymbol{Ey}^2 + \boldsymbol{Ez}^2$)$^{1/2}$) along y axis and z axis. $\boldsymbol{E}$ was large at the incident angle of 45° for both the bone model and the pipe-shaped model. Due to the attenuation of shear waves, $\boldsymbol{E}$ became smaller with propagation in the thickness direction. There is a slight increase in $\boldsymbol{E}$ in depth direction near the bottom, which may be due to shear waves generated by reflections from the bottom surface of the upper part of the bone.

4. Conclusion

The relationship between the electric field generated in bone and the angle of ultrasound incidence was investigated by simulation in order to improve the efficiency of ultrasonic bone fracture treatment. It was found that the electric field generated in the bone differs depending on the angle of ultrasound incidence. Considering the previously reported piezoelectric constants of bone, shear wave propagation may be a key factor.

Acknowledgment

This work was supported in part by the Uehara Memorial Life Science Foundation. The use of the human radius data was approved by the Human Ethics Review Committees at Doshisha University and Nagasaki University.

References

1. Friedenberg: J Bone Joint Surg Am. **53** (1971) 1400.
2. Fredericks: Orthop Trauma. **14** (2000) 93.
3. Inoue: J Orthop Res. **20** (2002) 1106.
4. Hosokawa: Jpn. J. Appl. Phys. **55** (2016) 07KF03.
5. Hata: Acoust. Soc. Am. **140** (2016) 3710.
6. Laugier, Haiat eds: Bone Quantitative Ultrasound, Springer, (2011).
7. Miyashita: J. Acoust. Soc. Am. Accepted.
8. Sasso: Ultrasound Med. Biol. **33** (2007) 1933
9. Nolle: J. Appl. Phys. **23** (1952) 888.

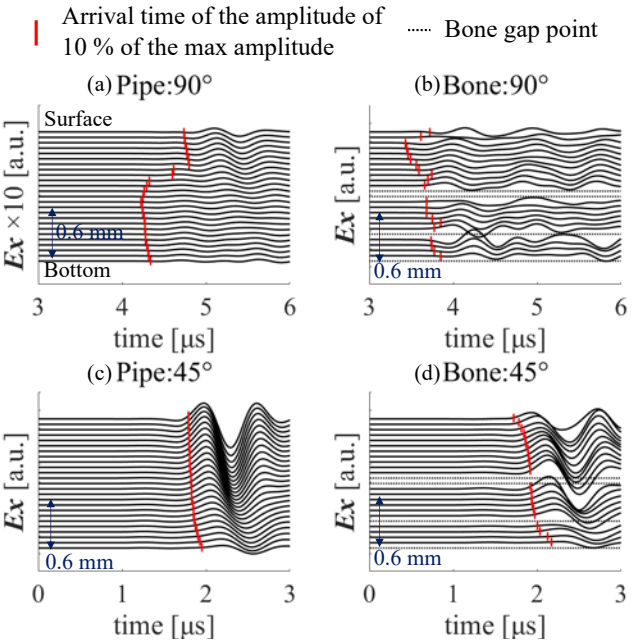

Fig. 2 Changes of *E*x along y axis direction in the upper part of the bone.

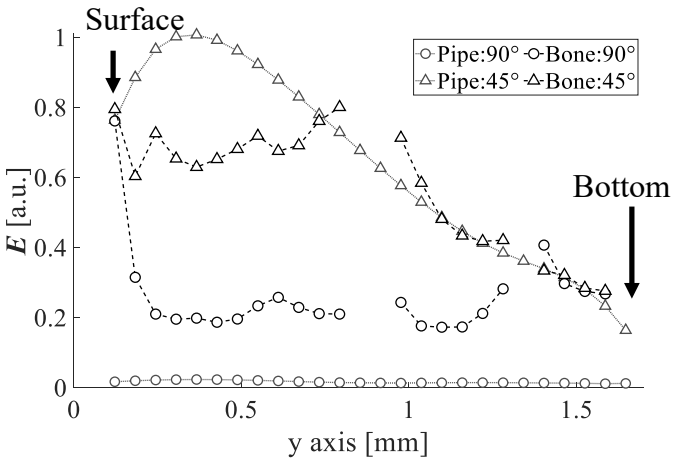

Fig. 3 Maximum electric field strength along y axis direction in the upper part of the bone.

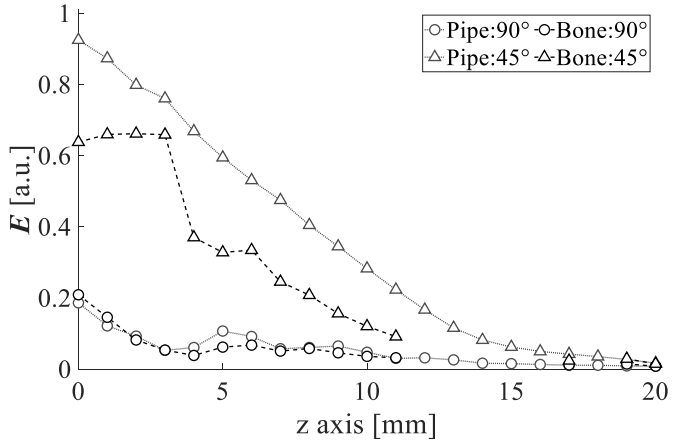

Fig. 4 Maximum electric field strength along z axis direction in the upper part of the bone.